



HAL
open science

Fast Compressive Raman Imaging of Polymorph Molecules and Excipients in Pharmaceutical Tablets

Clément Grand, Camille Scotté, Hervé Rigneault

► **To cite this version:**

Clément Grand, Camille Scotté, Hervé Rigneault. Fast Compressive Raman Imaging of Polymorph Molecules and Excipients in Pharmaceutical Tablets. *Analytical Chemistry*, 2022, 10.1021/acs.analchem.2c02680 . hal-03868911

HAL Id: hal-03868911

<https://hal.science/hal-03868911>

Submitted on 5 Mar 2023

HAL is a multi-disciplinary open access archive for the deposit and dissemination of scientific research documents, whether they are published or not. The documents may come from teaching and research institutions in France or abroad, or from public or private research centers.

L'archive ouverte pluridisciplinaire **HAL**, est destinée au dépôt et à la diffusion de documents scientifiques de niveau recherche, publiés ou non, émanant des établissements d'enseignement et de recherche français ou étrangers, des laboratoires publics ou privés.

Fast compressive Raman imaging of polymorph molecules and excipients in pharmaceutical tablets.

Clément Grand, Camille Scotté, and Hervé Rigneault*.

Aix Marseille Univ, CNRS, Centrale Marseille, Institut Fresnel, Marseille

*herve.rigneault@fresnel.fr

ABSTRACT: We implement a near infrared version (NIR) of compressive Raman imaging that incorporates a digital micro mirror device (DMD) and a single pixel detector for fast chemometric analysis and microscopic imaging. The NIR compressive Raman system is successfully used to detect and image active pharmaceutical ingredients exhibiting polymorphism within compact pharmaceutical tablets. We report the chemical imaging of a mixture of two clopidogrel polymorphs and three excipients in solid tablets with a pixel dwell time of 2.5 ms (0.5 ms per species). These results open the road to fast pharmaceutical tablet quality control imaging using compressive Raman technology.

Spontaneous Raman spectroscopy is a broadly recognized analytical technique spanning from research laboratories to industrial process lines¹. In the pharmaceutical industry Raman spectroscopy has found interests such as the analysis and quantification of active pharmaceutical ingredients (API)² but also in the pharmaceutical monitoring processes and in-line quality control³. Among the plethora of pharmaceutical applications of Raman spectroscopy, the detection and quantification of polymorph molecules (same chemical composition but different conformation) play a central role, because polymorph API often exhibit very different pharmaceutical efficiencies⁴. This can be explained knowing that the physicochemical properties of polymorph molecules differ, such as their solubility, dissolution kinetic, thermodynamic stability some leading to the dramatic alteration of their bio-availability and then their pharmaceutical efficiency⁵. Because conventional analytical techniques to detect polymorph such as X-rays powder diffraction and solid state nuclear magnetic resonance require complicated sample preparation and may find difficulties when probing the variety of compounds found in pharmaceutical dosages, Raman spectroscopy appeared as a rapid non-destructive appealing alternative⁶.

Ideally, Raman analysis should provide a spatially resolved maps for the API, including polymorphs, and the associated excipients necessary to ensure their bio-availability. However, Raman spectroscopy is often preferred over Raman imaging⁷ because the acquisition of the complete Raman spectrum for each sample spatial pixel, coupled with the weak Raman scattering cross section and detector array noise, requires lengthy acquisition times and generates large data sets. Typically, spontaneous Raman imaging requires 0.1 s per pixel leading rapidly to an over-night acquisition time (> 25 hours) to image a mm²

pharmaceutical tablet area with a spatial resolution of ~1micron⁸.

Notably, acquiring the complete Raman spectra at each sample pixel is a very inefficient way to map the spatial distribution of known pharmaceutical compounds. A more efficient way takes advantage of the knowledge of the molecular compounds that are present in a sample⁹. This precisely what does the recently developed compressive Raman technology (CRT)^{10, 11, 12, 13}. In CRT the measurement is directly designed to estimate the quantities of interest (*e.g.*, molecular concentrations), rather than deducing them from complete Raman spectra acquired at each pixel. Owing to the photon noise detection limit of single pixel detector and to the ability to retrieve the proportion estimation of chemical species with a low photons number, CRT was shown to perform Raman images $\times 10$ - $\times 100$ times faster than conventional EMCCD and CCD based Raman systems. Figure 1(a) shows a schematic view of a compressive Raman microscope¹⁴ where a digital micro mirror device (DMD), acting as a fast programmable binary spectral filter, is inserted into a spectrometer to send the Raman photons onto a single pixel detector^{10, 13}. Central to CRT are the design of the binary filters that are displayed sequentially to estimate the proportion of the chemical species, at each pixel (see Supp info paragraph 4 for a brief summary). The reported algorithms^{10, 12} proceed in a similar way to design filters that maximize the precision of the chemical species proportions. This is done by the minimization of the trace of covariance¹⁰, or the Cramer-Rao lower bound¹², matrices. The two approaches being equivalent when the number of binary filters equals the number of chemical species¹².

In here we follow the proportion estimation reported in¹² to map two polymorphs of clopidogrel, a commercial drug used to prevent platelet aggregation and to reduce heart disease risks and

strokes¹⁵, and three excipients (starch, mannitol and PEG) found commonly in pharmaceutical tablets. We show that these chemical species can be successfully estimated at each micron size location on the tablet surface with a pixel integration time as low as 2.5 ms (0.5 ms per species). This allows to map 1 mm² area in 40 minutes with a spatial resolution of 1 μm .

EXPERIMENTAL SECTION

Compressive Raman Technology (CRT): The complete CRT setup is shown in supporting information figure S1. It uses a 785nm CW laser (IPS – 100mW) to minimize parasitic fluorescence with a laser line filter integrated to reduce the bandwidth down to 0.3 cm^{-1} , a two axis galvanometric scanner (Cambridge Technology) and a commercial microscope stand (Nikon Eclipse) equipped with a $\times 20$, NA = 0.75 objective lens (Nikon CFI Apo Lambda). This objective focuses the 785 nm excitation light and collects the back emitted/reflected Raman photons. The latter are descanned and separated from the excitation beam by a dichroic mirror and sent to a custom build CRT spectrometer. At the spectrometer entrance a 785 nm notch filter (HSPF785.0 – Kaiser) reject all the remaining laser and Rayleigh light. The CRT spectrometer is composed of a high transmission (~85%) grating (1200 groove/mm) that dispersed the Raman photons towards the DMD (Vialux V-650L NIR) with optimized NIR reflection. The binary encoded spectral filter displayed on the DMD send the Raman photons towards a single photon avalanche photodiode (SPAD-ID Quantique-ID120) with a 75% quantum efficiency at 800nm. The galvo mirrors control and image acquisition is controlled by a custom Lab-View based software. This software controls also the DMD display via the Vialux interface. To end this paragraph, in our case, the spectral resolution is estimated to be $\delta\lambda \approx 12 \text{ cm}^{-1}$, the spatial resolution 1 μm (x,y) and 10 μm (z axis).

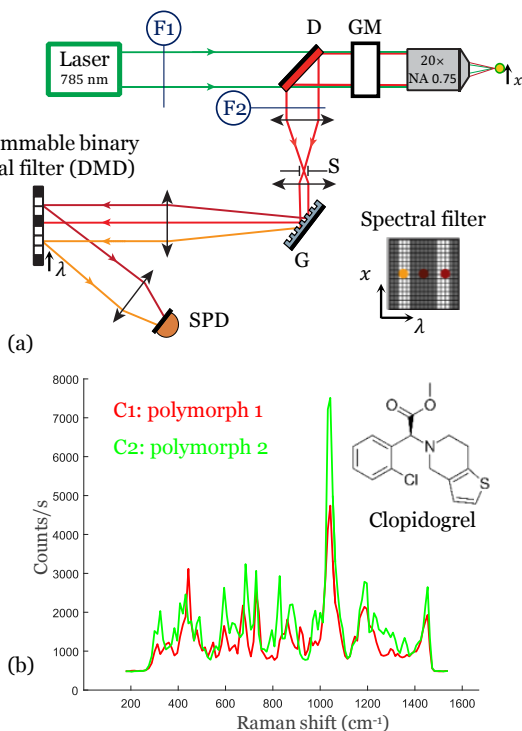


Figure 1. (a) Simplified sketch of a CRT setup (see supp info for a detailed setup description), in this work we developed a NIR CRT

version with a laser emitting at 785 nm; D: dichroic mirror; GM: Galvanometric mirrors; S: confocal slit; G: amplitude grating (1200 lines/mm); DMD: digital micro mirror device; SPD: single pixel detector; F1: laser line filter, F2: notch filter. **(b)** Spontaneous Raman spectra of the two polymorph forms C1 (red) and C2 (green) of clopidogrel.

Polymorph CRT imaging: To illustrate the relevance of CRT to image APIs in tablets we choose two polymorph forms called C1 and C2. The spontaneous Raman spectra of C1 and C2 are shown in Figure 1(b). These known spectra are used to design the binary filters that minimize the variance of the estimated C1 and C2 proportions following^{12, 13}. The designed binary filters are displayed in Figure 2 (a, b) for the two polymorph forms C1 and C2, respectively (Raman photons falling in the white stripes are kept while the photons falling in the grey stripes are rejected).

The CRT proportion estimate^{12, 13} of C1 and C2 mixed in a test pharmaceutical tablet have been associated with an RGB filter and shown in Figure 2(c). When colored in red (C1) and green (C2) (Fig. 2(c)) and overlaid (Fig. 2(d)), they provided a colorful chemical image of the two polymorph distributions in the measured tablet. Figure 2(c) presents the proportion estimate of the C1 and C2 species. The background (in black) is also considered as a species and has its own binary filter (not shown). From the three species (C1, C2, background) proportions present at each pixel, a classification is carried out: on Fig. 2(d), at each pixel, a single color is displayed that corresponds to the dominant species. This classification is justified because the tablet has been produced from pure C1 and C2 compounds. Note that no further image processing (smoothing...) was performed to improve the image rendering.

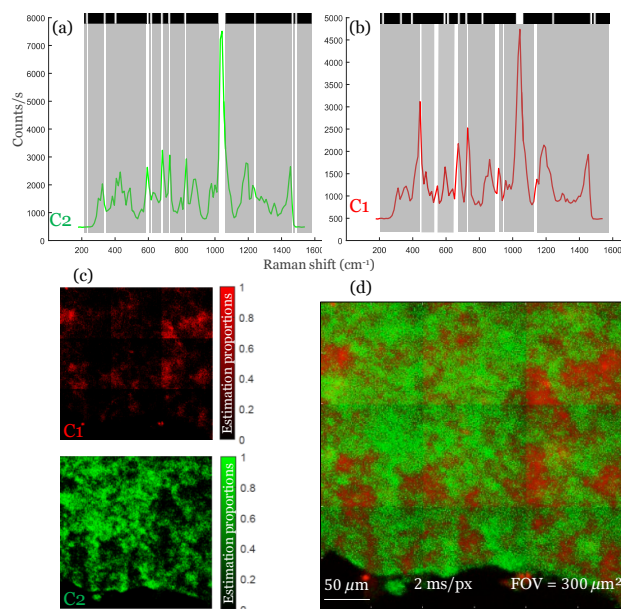


Figure 2. Designed binary filters (Raman photons falling in the white stripes are kept while the photons falling in the grey stripes are rejected) for clopidogrel polymorphs C1 **(a)** and C2 **(b)**. **(c)** Portion estimates for C1 and C2 as retrieved by the algorithm and colored in red (C1) and green (C2) using an RGB filter. **(d)** The overlaid of the two provides chemical imaging of the tablet (the image scan was performed near the tablet edge for clarity). Scale bar: 50

μm , pixel dwell time for each API image: 5 ms (10 ms in total), $300 \times 300 \mu\text{m}$ (300×300 pixels)

Polymorph and excipient CRT imaging: Next we consider a powder mixture composed of the C1 and C2 clopidogrel polymorphs mixed with three excipients: starch (STA), mannitol (MAN) and polyethylene glycol (PEG). The powder chemical compounds were deposited on a CaF_2 substrate without further preparation and directly imaged with the compressive Raman microscope. Figure 3(a) shows the Raman spectra of the five considered species together with the numerically designed binary filters (top rows – white pixels correspond to selected wavenumbers whereas black pixels correspond to rejected wavenumbers). Figure 3(b) displays the estimated proportions (that have been colored filtered) for each of the APIs and overlaid on the same image. All the APIs could be identified correctly and the proportion algorithms could retrieve the pure nature of the powder samples (each of the pixel is a pure chemical species). Note that at certain zones in the image, we see superposition of C1 and C2, which may not be fully identified spatially. We can assume that at these points a higher number of photon (and therefore a longer acquisition time) would be necessary in order to be able to perfectly discriminate between these two spectrally very close species. In supp info Fig. S2 we validate the CRT species identifications for 5 species by recording full Raman spectra. This validates the chemical species validated by CRT.

Complex pharmaceutical tablet imaging: As a final example we consider a compact tablet (1.5 cm diameter, ~ 2 mm thick) made of the two clopidogrel polymorphs and the three excipients in the relative proportion 10% C1, 40% C2, 40% STA, 5% MAN and 5% PEG. The five binary filters used for CRT imaging were the same as in figure 3 and demonstrate the ability of CRT to work with binary filters that have been designed once (Fig. 3(a)) and hold for further measurements. Figure 4 shows the estimation proportion of the three most concentrated APIs (C1, C2 and STA) over a region of interest of $300 \times 300 \mu\text{m}$ located near the edge of the tablet. Note the chemical species MAN and PEG couldn't be found in this region. As in figure 2(d) and 3(b), no further image processing was performed to improve the image rendering.

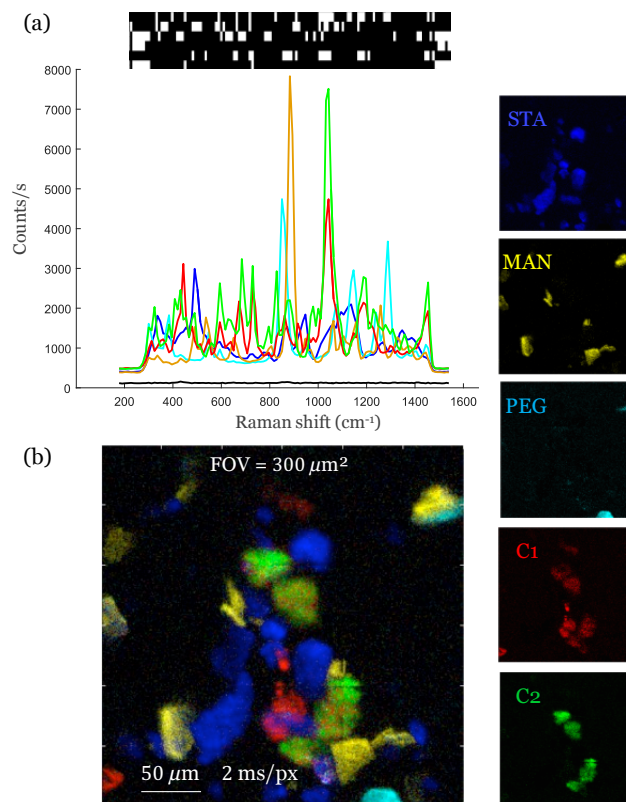


Figure 3. Powder samples: (a) Raman spectra of the five considered API, C1 and C2: clopidogrel polymorphs, STA: starch, MAN: mannitol, PEG: polyethylene glycol and the associated five binary filters. (b) Estimation proportions color filtered and overlaid on the same image. Scale bar $50 \mu\text{m}$, pixel dwell time for each species image 2 ms, $300 \times 300 \mu\text{m}$ (300×300 pixels).

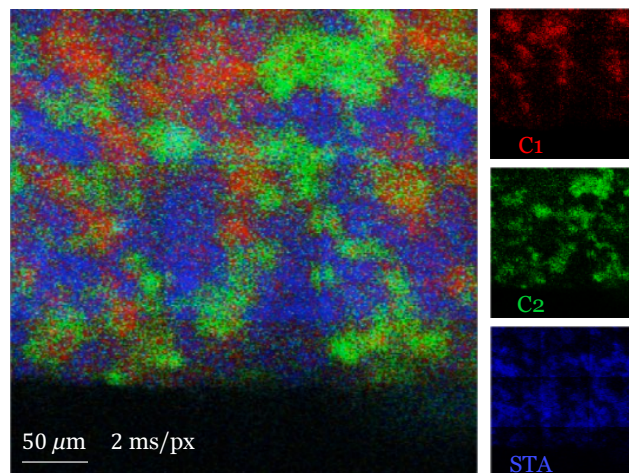


Figure 4: Complex pharmaceutical compact tablet composed of 10% C1, 40% C2, 40% STA, 5% MAN and 5% PEG as imaged by CRT. Only C1, C2 and STA could be retrieved in this region of interest located close to the tablet edge. Scale bar $50 \mu\text{m}$, pixel dwell time for each species image 2 ms, $300 \times 300 \mu\text{m}$ (300×300 pixels)

High speed pharmaceutical tablet CRT imaging: For this type of application where the compounds are *a priori* known, CRT is beneficial over conventional Raman because it uses

prior information on the chemical species Raman spectra from which the binary filters can be designed (Fig. 2(a) and 3(a)). To investigate the ability of our CRT setup to perform fast imaging of complex pharmaceutical tablets figure 5 compares the CRT image quality obtained with pixel dwell time ranging from 0.5 ms/pix to 10 ms/pix. The considered API sample and the region of interest is the same as in figure 4 (complex tablet). At 0.5 ms/pixel/species it is still possible to distinguish the three chemical species C1, C2 and STA. This probably sets the speed limit on this type of sample to access a decent signal-to-noise ratio for API detection. We noted that for increasing pixel dwell time, the error probability decreases and the estimator reveals the accurate chemical species at each pixel. As a consequence, with increasing pixel dwell time, there are more and more pixels that take the same color on macroscopic areas that correspond to a pure chemical compound.

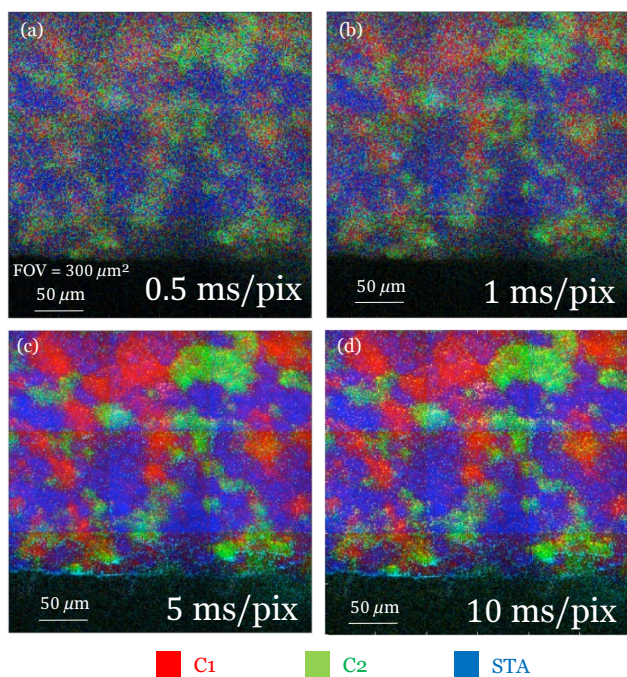


Figure 5. CRT imaging performed at different pixel dwell time. (a) 0.5 ms/pixel/species, (b) 1ms/pixel/species, (c) 5 ms/pixel/species and (d) 10 ms/pixel/species. C1 and C2: clopidogrel polymorphs, STA: starch. $300 \times 300 \mu\text{m}$ (300×300 pixels).

CRT comparison with stimulated Raman imaging: As an interesting comparison in reference¹⁶ we used stimulated Raman¹⁷ to image in Epi collection the same tablet samples with a pixel dwell time of $400 \mu\text{s}$ per spectral point. Although a precise comparison between CRT and SRS is difficult we qualitatively estimate that the CRT image quality at 5 ms/pixel is similar to the SRS image quality at 0.4 ms/pixel. This make SRS superior by roughly a factor of 10 as compared to CRT for this type of compact pharmaceutical tablet samples; an advantage that comes at the price of a drastic increase in technological complexity for SRS (ultra-fast lasers, lock-in detection...)^{16, 18}. Note that with improved Epi detection SRS can provide chemical images with a pixel dwell time as short as 100 ns ¹⁹.

DISCUSSION AND CONCLUSION

In this work, we have developed a NIR (785 nm) CRT using galvo scanners to quickly scan a focused laser beam across the sample. The CRT imaging system uses a DMD to display sequentially the optimally designed binary filters¹² for each scanned region of interest. This enables chemical proportion estimation of API across the imaging area with a transverse resolution of $\sim 1 \mu\text{m}$ and a longitudinal resolution of $\sim 5 \mu\text{m}$. We have used this system to map APIs in compact pharmaceutical tablets among which two polymorphs show very similar Raman spectra (Fig 1(b)). We have successfully demonstrated the ability of CRT to estimate the chemical proportion for each polymorph and excipient at each pixel. This can be confirmed by performing a quick spectral scan using the DMD for each estimated pure chemical species (Supplementary figure S2). We have demonstrated that the imaging speed can be pushed up to 0.5 ms/pixel/species (2.5 ms in total for 5 species) (Fig. 5(a)) to map a mixture of complex APIs such as polymorphs and excipient in tablets. This leads to image a $300 \times 300 \mu\text{m}$ region of interest in 45 s per species (~ 4.5 minutes for 5 chemical species). By stitching the field of view our current CRT system can image a 1 mm^2 tablet area in 40 minutes with a resolution of $1 \mu\text{m}$ (Supplementary figure S3). These results suggest that CRT is a valuable alternative technology for pharmaceutical active ingredient mapping with potential application in fast in-line quality control

Supporting Information

The supplementary information includes:

Figure S1: detailed description of the CRT experimental setup

Figure S2: spectral validation of the estimated species

Figure S3: CRT image of 1 mm^2 tablet sample area.

AUTHOR INFORMATION

Corresponding Author

Hervé Rigneault (hervé.rigneault@fresnel.fr)

Author Contributions

CG, CS and HR designed and built the experiment, CS and CG performed the measurements and the data analysis. The manuscript was written by CG and HR and approved by all authors.

The authors declare no conflict of interest

ACKNOWLEDGMENT

The authors thank Valérie Lavastre, Jean Alie, and Géraldine Pénardier from Sanofi (Montpellier – France) for providing the active pharmaceutical ingredients samples.

The authors acknowledge the support of the Centre National de la Recherche Scientifique (CNRS), Agence Nationale de la Recherche (ANR-21-ESRS-0002 IDEC).

REFERENCES

- (1) Lewis, I. R. E. H. G. M. *Handbook of Raman spectroscopy : from the research laboratory to the process line*; Marcel Dekker, 2001.
- (2) Gendrin, C.; Roggo, Y.; Collet, C. Pharmaceutical applications of vibrational chemical imaging and chemometrics: a review. *J Pharm Biomed Anal* **2008**, *48* (3), 533-553. DOI: 10.1016/j.jpba.2008.08.014 From Nlm.
- (3) Févotte, G. In Situ Raman Spectroscopy for In-Line Control of Pharmaceutical Crystallization and Solids Elaboration Processes: A Review *Chemical Engineering Research and Design* **2007**, *85* (7), 906-920.
- (4) Bauer, J. F. Polymorphism—A Critical Consideration in Pharmaceutical Development, Manufacturing, and Stability. *J. Valid. Technol.* **2008**, 15-23.
- (5) Censi, R.; Di Martino, P. Polymorph Impact on the Bioavailability and Stability of Poorly Soluble Drugs. *Molecules* **2015**, *20* (10), 18759-18776. DOI: 10.3390/molecules201018759 PubMed.
- (6) Feng, H.; Bondi, R. W., Jr.; Anderson, C. A.; Drennen, J. K., 3rd; Igne, B. Investigation of the Sensitivity of Transmission Raman Spectroscopy for Polymorph Detection in Pharmaceutical Tablets. *Appl Spectrosc* **2017**, *71* (8), 1856-1867. DOI: 10.1177/0003702817690407 From Nlm. Strachan, C. J.; Rades, T.; Gordon, K. C.; Rantanen, J. Raman spectroscopy for quantitative analysis of pharmaceutical solids. *The Journal of pharmacy and pharmacology* **2007**, *59* (2), 179-192. DOI: 10.1211/jpp.59.2.0005 From Nlm.
- (7) Roggo, Y.; Degardin, K.; Margot, P. Identification of pharmaceutical tablets by Raman spectroscopy and chemometrics. *Talanta* **2010**, *81* (3), 988-995. DOI: 10.1016/j.talanta.2010.01.046 From Nlm.
- (8) Carruthers, H.; Clark, D.; Clarke, F.; Faulds, K.; Graham, D. Comparison of Raman and Near-Infrared Chemical Mapping for the Analysis of Pharmaceutical Tablets. *Appl Spectrosc* **2021**, *75* (2), 178-188. DOI: 10.1177/0003702820952440 From Nlm.
- (9) Cebeci Maltaş, D.; Kwok, K.; Wang, P.; Taylor, L. S.; Ben-Amotz, D. Rapid classification of pharmaceutical ingredients with Raman spectroscopy using compressive detection strategy with PLS-DA multivariate filters. *Journal of Pharmaceutical and Biomedical Analysis* **2013**, *80*, 63-68. DOI: <https://doi.org/10.1016/j.jpba.2013.02.029>.
- (10) Wilcox, D. S.; Buzzard, G. T.; Lucier, B. J.; Wang, P.; Ben-Amotz, D. Photon level chemical classification using digital compressive detection. *Analytica chimica acta* **2012**, *755*, 17-27. DOI: 10.1016/j.aca.2012.10.005 From Nlm.
- (11) Wilcox, D. S.; Buzzard, G. T.; Lucier, B. J.; Rehrauer, O. G.; Wang, P.; Ben-Amotz, D. Digital compressive chemical quantitation and hyperspectral imaging. *Analyst* **2013**, *138* (17), 4982-4990, 10.1039/C3AN00309D. DOI: 10.1039/C3AN00309D. Cebeci, D.; Mankani, B. R.; Ben-Amotz, D. Recent Trends in Compressive Raman Spectroscopy Using DMD-Based Binary Detection. *Journal of Imaging* **2018**, *5* (1), 1. Rehrauer, O. G.; Dinh, V. C.; Mankani, B. R.; Buzzard, G. T.; Lucier, B. J.; Ben-Amotz, D. Binary Complementary Filters for Compressive Raman Spectroscopy. *Appl. Spectrosc.* **2018**, *72* (1), 69-78. Réfrégier, P.; Chevallier, E.; Galland, F. Compressed Raman classification method with upper-bounded error probability. *Optics Letters* **2019**, *44* (23), 5836-5839. DOI: 10.1364/OL.44.005836. Justel, T.; Galland, F.; Roueff, A. Compressed Raman method combining classification and estimation of spectra with optimized binary filters. *Optics Letters* **2022**, *47* (5), 1101-1104. DOI: 10.1364/OL.447769.
- (12) Réfrégier, P.; Scotté, C.; de Aguiar, H. B.; Rigneault, H.; Galland, F. Precision of proportion estimation with binary compressed Raman spectrum. *Journal of the Optical Society of America A* **2018**, *35* (1), 125-134. DOI: 10.1364/JOSAA.35.000125.
- (13) Scotté, C.; de Aguiar, H. B.; Marguet, D.; Green, E. M.; Bouzy, P.; Vergnole, S.; Winlove, C. P.; Stone, N.; Rigneault, H. Assessment of Compressive Raman versus Hyperspectral Raman for Microcalcification Chemical Imaging. *Analytical Chemistry* **2018**, *90* (12), 7197-7203. DOI: 10.1021/acs.analchem.7b05303.
- (14) Sturm, B.; Soldevila, F.; Tajahuerce, E.; Gigan, S.; Rigneault, H.; de Aguiar, H. B. High-Sensitivity High-Speed Compressive Spectrometer for Raman Imaging. *ACS Photonics* **2019**, *6* (6), 1409-1415. DOI: 10.1021/acsphotonics.8b01643.
- (15) Bates, E. R.; Lau, W. C.; Angiolillo, D. J. Clopidogrel-drug interactions. *Journal of the American College of Cardiology* **2011**, *57* (11), 1251-1263. DOI: 10.1016/j.jacc.2010.11.024 From Nlm. Price, M. J.; Walder, J. S.; Baker, B. A.; Heiselman, D. E.; Jakubowski, J. A.; Logan, D. K.; Winters, K. J.; Li, W.; Angiolillo, D. J. Recovery of platelet function after discontinuation of prasugrel or clopidogrel maintenance dosing in aspirin-treated patients with stable coronary disease: the recovery trial. *Journal of the American College of Cardiology* **2012**, *59* (25), 2338-2343. DOI: 10.1016/j.jacc.2012.02.042 From Nlm.
- (16) Sarri, B.; Canonge, R.; Audier, X.; Lavastre, V.; Pénarier, G.; Alie, J.; Rigneault, H. Discriminating polymorph distributions in pharmaceutical tablets using stimulated Raman scattering microscopy. *Journal of Raman Spectroscopy* **2019**, *50* (12), 1896-1904. DOI: 10.1002/jrs.5743.
- (17) Rigneault, H.; Berto, P. Tutorial: Coherent Raman light matter interaction processes. *APL Photonics* **2018**, *3* (9), 091101. DOI: 10.1063/1.5030335 (accessed 2018/07/27).
- (18) Heuke, S.; Rimke, I.; Sarri, B.; Gasecka, P.; Appay, R.; Legoff, L.; Volz, P.; Büttner, E.; Rigneault, H. Shot-noise limited tunable dual-vibrational frequency stimulated Raman scattering microscopy. *Biomed. Opt. Express* **2021**, *12* (12), 7780-7789. DOI: 10.1364/BOE.446348.

(19) Saar, B. G.; Freudiger, C. W.; Reichman, J.; Stanley, C. M.; Holtom, G. R.; Xie, X. S. Video-rate molecular imaging in vivo with stimulated Raman scattering. *Science* **2010**, *330* (6009), 1368-1370.
